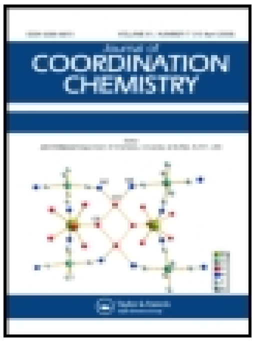

Journal of Coordination Chemistry

ISSN: 0095-8972 (Print) 1029-0389 (Online) Journal homepage: http://www.tandfonline.com/loi/gcoo20

Chromotropism in halo-bridged dimers. Structural characterization of bis(μ-halo)bis(halo N-(pyridin-2-ylmethyl)cyclohexanamine copper(II))

Hamid Golchoubian & Samira Nateghi

To cite this article: Hamid Golchoubian & Samira Nateghi (2016): Chromotropism in halo-bridged dimers. Structural characterization of bis(μ-halo)bis(halo N-(pyridin-2-ylmethyl)cyclohexanamine copper(II)), Journal of Coordination Chemistry, DOI: 10.1080/00958972.2016.1227972

To link to this article: http://dx.doi.org/10.1080/00958972.2016.1227972

JOURNAL OF COORDINATION CHEMISTRY, 2016
http://dx.doi.org/10.1080/00958972.2016.1227972

Chromotropism in halo-bridged dimers. Structural characterization of bis(μ-halo)bis(halo N-(pyridin-2-ylmethyl) cyclohexanamine copper(II))

Hamid Golchoubian and Samira Nateghi

Department of Chemistry, University of Mazandaran, Babol-sar, Iran

ABSTRACT

Two dinuclear copper(II) complexes, [LCu(μ-Cl)Cl]$_2$ (DMF) (**1**) and [LCu(μ-Br)Br]$_2$ (**2**), with the bidentate ligand *N*-(pyridin-2-ylmethyl)cyclohexanamine, L, were synthesized and characterized by physicochemical and spectroscopic (IR, UV–vis) data. The crystal structural analysis of **1** shows that both copper(II) ions are in a distorted square pyramidal N_2Cl_3 environment with the apical position of the copper(II) being occupied by the bridging chloride anion which is equatorial to the other copper ion, forming a dimeric copper(II) complex. The chromotropic properties of both complexes, including solvato-, thermo-, and halochromism, were investigated. The complexes show reversible thermochromism in solution which is irreversible in the solid state. It was found that the solvatochromism is due to structural change followed by solvation of the vacant sites of the complexes. Their halochromic properties were studied in pH range of 1–11 by visible absorption spectroscopy. The color changes from blue to green and to colorless are due to deprotonation and protonation of the ligands.

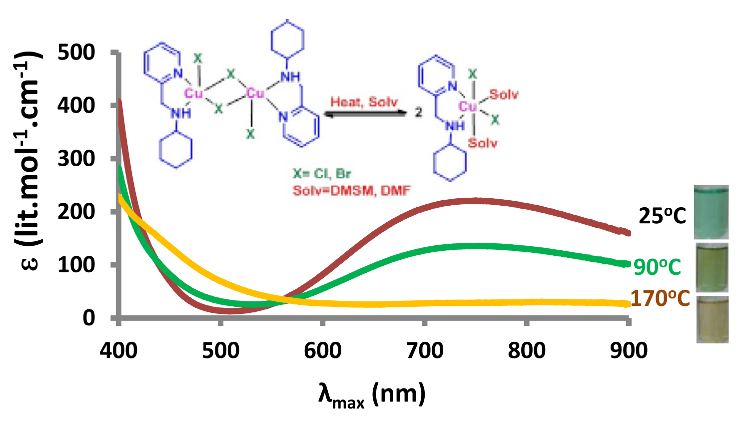

ARTICLE HISTORY
Received 8 April 2016
Accepted 27 June 2016

KEYWORDS
Dinuclear copper(II); bis(μ-chloro)-bridge; chromotropism; pyridine derivative; crystal structure

CONTACT Hamid Golchoubian ✉ h.golchobian@umz.ac.ir

Supplemental data for this article can be accessed at http://dx.doi.org/10.1080/00958972.2016.1227972.

1. Introduction

Chromotropism is the reversible color transformation of materials due to surrounding physical and chemical conditions such as temperature (thermochromism), solvent (solvatochromism), ion (ionochromism), pH (halochromism), pressure (piezochromism), light (photochromism), and electro-redox reaction (electrochromism) [1]. The development of an empirical relationship that correlates the structural characteristics of transition metal complexes to their chromotropism properties has been vigorously pursued [1–6]. Studies of this kind have provided significant results in a variety of complexes [7–11]. Among the transition metal complexes, copper(II) ions with chelate ligands have been recognized as the most encouraging candidates for practical applications of chromotropism due to their high thermodynamic stabilities, unsaturated coordination, and also the existence of simple and regular changes in their electronic spectra in accordance with the power of the stimuli imposed to the system.

Dinuclear copper(II) compounds with small anions (such as halide or hydroxide) as bridging groups are the subject of numerous articles in contemporary literature [12–42]. The study of these dinuclear complexes is complicated, partly due to their diverse structural properties. The $[Cu(\mu\text{-}X)_2Cu]$ dimeric motif, where X is Cl^- or Br^-, exhibits structures with a variety of Cu–X lengths and Cu–X–Cu angles depending upon the nature of the co-ligands and also on the counter ions [23, 43]. So far, various types of bidentate organic co-ligands have been utilized to design the coordination sphere of the copper(II) center in bis(μ-halo)-bridged complexes [34, 35, 38, 44–46]. However, the number of halo-bridged complexes involving bidentate pyridine derivative co-ligands is very limited [13, 47–49]. We have recently been focusing our attention on five-coordinate dimeric species, and here, also, there is a range of geometries from tetragonal-pyramidal to trigonal-bipyramidal at copper. In view of our interest in chromotropism of copper(II) compounds, we wished to extend our work to dinuclear copper(II) halide complexes in combination with a bidentate pyridine derivative, *N*-(pyridin-2-ylmethyl)cyclohexanamine (L; scheme 1). We have isolated and characterized neutral dinuclear copper(II) chloro and bromo complexes, $[LCu(\mu\text{-}X)X]_2$ (X = Cl, Br). Details of the synthesis, crystal structure, and chromotropism behaviors of these compounds are described below.

2. Experimental

2.1. Materials and methods

$CuCl_2 \cdot 2H_2O$ and $CuBr_2$ were purchased from Merck India Ltd and Fluka Chemie Switzerland, respectively, and 2-pyridinecarboxaldehyde and cyclohexylamine were purchased from Sigma–Aldrich, USA. All chemicals and solvents employed for the syntheses were of analytical grade and used as received. All solvents used for chromotropism studies were spectral-grade and all other reagents were used as received. Elemental analyses were performed on a LECO CHN-600 Elemental Analyzer. Absolute metal percentages were determined by a Varian-spectra A-30/40 atomic absorption flame spectrometer. All samples were dried to constant weight under a high vacuum prior to analysis. Conductance measurements were

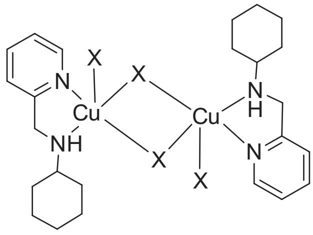

Scheme 1. Dinuclear complexes under study.

made at 25 °C with a Jenway 400 conductance meter on concentrations of 10.0×10^{-4}, 6.00×10^{-4}, 4.00×10^{-4} and 2.00×10^{-4} M of samples in selected solvents. Then for each solvent, a curve was plotted by plotting the molar conductance *versus* concentration of sample. The curve was then extrapolated to an infinitively dilute solution to obtain the molar conductance value. Infrared spectra were recorded using potassium bromide disks and a Bruker FT-IR instrument. NMR spectra were measured with a Bruker 400 DRX Fourier Transform Spectrometer at room temperature. The electronic absorption spectra were measured with a Braic2100 UV–vis spectrophotometer. The following solvents were used in the solvatochromism study: nitromethane (NM), nitrobenzene (NB), acetone (AC), acetonitrile (AN), propionitrile (PN), methanol (MeOH), ethanol (EtOH), water (H_2O), dimethylformamide (DMF), dimethylsulfoxide (DMSO), and hexamethylphosphorictriamide (HMPA).

2.2. Synthesis

2.2.1. Preparation of N-(pyridin-2-ylmethyl)cyclohexanamine (L)

A mixture of pyridine-2-carbaldehyde (2.9 mL, 30 mmol), cyclohexylamine (3.4 mL, 30 mmol), and a small amount of *para*-toluenesulfonic acid in methanol (35 mL) was prepared and stirred for one day at room temperature. $NaBH_4$ (1.7 g, 45 mmol) was then added gradually to the resulting solution over 30 min. The resulting mixture was allowed to stand overnight. After heating the solution near the boiling point, HCl (10 mL, 1.7 M) was added to it after placing the solution in an ice bath and was then heated again to the boiling temperature. The mixture was then made alkaline by addition of NaOH (4 M). The sodium borate precipitate was removed by filtration. Evaporation of the solvent from the filtrate resulted in a yellow oil which was subsequently extracted with dichloromethane (3 × 15 mL). The combined CH_2Cl_2 fractions were dried over anhydrous Na_2SO_4. Evaporation of the solvent under reduced pressure resulted in the desired product as a brown oil. The yield was 3.71 g (64%). Selected IR data (v/cm^{-1} using KBr disk): 3307 (m, N–H str.), 2927, 2853 (s, C–H str. aliphatic), 1593 (s, C=N str.), 1438 (s, C=C str. aromatic), 1227 (s, N–C str. aliphatic). ^{1}H NMR (400 MHz, $CDCl_3$), δ: 1.17 (m, 5H, (cyclohexyl–); 1.57 (m, 2H, (cyclohexyl–)); 1.70 (m, 2H, (cyclohexyl–)); 1.90 (m, 1H, (cyclohexyl–)); 2.45 (m, 1H, (cyclohexyl–)); 2.57 (br. H, –NH–); 3.89 (s, 2H, –C**H**$_2$–Py); 7.11 (d,d, $J = 5.6, 1.6$ Hz, H, Py); 7.27 (s, H, Py); 7.58 (t,d, $J = 7.6, 2.0$ Hz, H, Py); 8.50 (d, $J = 4.4$ Hz, H, Py). When one drop of D_2O was added to the ^{1}H NMR sample, the broad signal at 2.57 ppm disappeared. ^{13}C NMR (100 MHz in $CDCl_3$), δ: 24.97, 26.19,33.42, 56.55 (cyclohexyl–); 52.27 (–NH–$\underline{C}H_2$–Py); 121.83; 122.36.136.42, 149.17, 159.97 (Py–C).

2.2.2. Preparation of bis((μ-chloro)chloro, N-(pyridin-2-ylmethyl)cyclohexanamine copper(II)) dimethylformamide, [LCu(μ-Cl)Cl]$_2$ DMF (**1**)

To a solution of *N*-(pyridin-2-ylmethyl)cyclohexanamine, L (0.38 g, 2 mmol) in ethanol (12 mL) was slowly added a solution of $CuCl_2 \cdot 2H_2O$ (0.34 g, 2 mmol) in ethanol (8 mL). The resulting green mixture was stirred for 2 h at room temperature and was then allowed to concentrate at room temperature. The desired compound precipitated from the solution as a greenish blue solid. The compound was recrystallized by diffusion of diethyl ether into a DMF solution. Yield 0.57 g, 78% as blue-green crystals. The crystals were suitable for X-ray crystallography. Anal. Calcd for $C_{27}H_{43}N_5Cu_2Cl_4O$ (MW = 722.57 g mol^{-1}): C, 44.88; H, 6.00; N, 9.69; Cu, 17.59%; Found: C, 44.91; H, 6.09; N, 9.77; Cu, 17.41%. Selected IR data (*v*/cm^{-1} using KBr disk): 3427 (m), 3196 (m, N–H str.), 3072 (w), 2931, 2852 (s C–H str.), 1608 (s, C=N str.), 1448 (m, N–H bend.), 1287 (w), 771(m), 651 (w).

2.2.3. Preparation of bis((μ-bromo)bromo, N-(pyridin-2-ylmethyl)cyclohexanamine copper(II)) [LCu(μ-Br)Br]$_2$ (**2**)

This complex was prepared by a similar method to that used for [LCu(μ-Cl)Cl]$_2$, except that $CuBr_2$ was used (0.45 g) in place of $CuCl_2 \cdot 2H_2O$. The compound was obtained as a dark green solid with typical yield of 64% (0.53 g based on 2 mmol $CuBr_2$ used). Anal. Calcd for $C_{24}H_{36}N_4Cu_2Br_4$ (MW = 827.28 g mol^{-1}): C, 34.84; H, 4.39; N, 6.77; Cu, 15.36%; Found: C, 34.89; H, 4.20; N, 6.74; Cu, 15.52 %. Selected IR data

(v/cm^{-1} using KBr disk): 3203 (m, N–H str.), 3062 (w), 2928, 2853 (s C–H str.), 1592 (s, C=N str.), 1438 (m, N–H bend.), 1301 (w), 754(m), 663 (w).

2.3. X-ray crystallographic study

X-ray data for **1** were collected on a STOE IPDS-II diffractometer with graphite monochromated Mo-Kα radiation. A green crystal of the complex was chosen using a polarizing microscope and was mounted on a glass fiber which was used for data collection. Cell constants and an orientation matrix for data collection were obtained by least squares refinement of diffraction data from 7160 unique reflections. Data were collected at 298(2) °C in a series of ω scans in 1° oscillations and integrated using the Stöe X-AREA [50] software package. A numerical absorption correction was applied using XRED [51] and X-SHAPE [52] software. The data were corrected for Lorentz and polarizing effects. The structure was solved by direct methods using SIR2004 [53]. The non-hydrogen atoms were refined anisotropically by full matrix least squares on F^2 using SHELXL [54]. All hydrogens were added at ideal positions and constrained to ride on their parent atoms. Crystallographic data are listed in table 1.

3. Results and discussion

3.1. Preparation

The ligand was prepared by condensation of an equimolar mixture of cyclohexylamine and pyridine-2-carbaldehyde and further reduction of the resultant diimine by sodium borohydride. The dinuclear copper(II) complex was synthesized by mixing an equimolar quantity of $CuCl_2\cdot 2H_2O$ or $CuBr_2$ and the ligand in ethanol in moderate yields (scheme 2).

Table 1. Crystal data and structure refinement for **1**.

Empirical formula	$C_{27}H_{43}Cl_4Cu_2N_5O$
Formula weight	722.54
Shape, color	Prism, green
Temperature	298(2) K
Wavelength	0.71073 Å
Crystal system	Monoclinic
Space group	*P21/c*
Unit cell dimensions	
a	12.491(3) Å
b	13.338(3) Å
c	19.756(4) Å
β	92.85(3)°
Volume	3287.3(13) Å^3
Z	4
Calculated density	1.460 g cm^{-3}
Absorption coefficient	1.648 mm^{-1}
F (0 0 0)	1496
Crystal size	0.35 × 0.25 × 0.15 mm^3
θ range for data collection	2.57°–27.00°
Index ranges	$-15 \le h \le 15$
	$-17 \le k \le 15$
	$-25 \le l \le 25$
μ (mm^{-1})	1.648
Reflections collected/unique	22,454/7160 [*R*(int) = 0.0348]
Completeness to $2\theta = 27.00$	99.9%
Refinement method	Full-matrix least-squares on F^2
Data/restraints/parameters	7160/0/362
Final *R* indices[a] $[I > 2\sigma(I)]$[b]	$R_1 = 0.0332$, $wR_2 = 0.0850$
Goodness-of-fit on F^2[c]	0.978
R indices (all data)	$R_1 = 0.0466$, $wR_2 = 0.0887$
Largest diff. peak and hole	0.212 and −0.249 e Å^{-3}

[a] $R = \Sigma||F_o| - |F_c||/\Sigma|F_o|$.
[b] $wR = [(\Sigma[F_o^2 - F_c^2)^2]/\Sigma[w(F_o^2)^2]]^{1/2}$.
[c] $S = \Sigma[w(F_o^2 - F_c^2)^2/(N_{obs} - N_{param})]^{1/2}$.

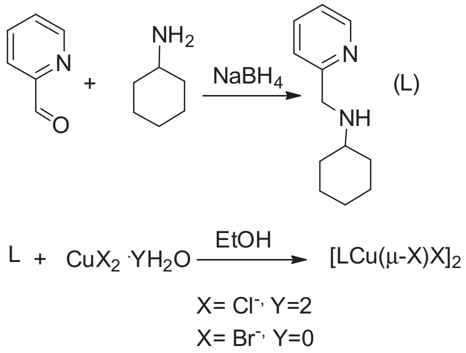

Scheme 2. Synthetic outline for preparation of ligands and complexes.

3.2. Characterization

The free ligand has characteristic IR bands with minor shifts in the dinuclear complexes. A medium intensity and narrow band at 3307 cm^{-1} is associated with the N–H stretch of the amine group. Upon formation of the chelate rings in the complexes, this band moves to lower energy (3196 and 3203 cm^{-1} in **1** and **2**, respectively). As the lone pair of electrons of the donor nitrogen becomes involved in the metal-ligand bond, the transfer of electron density to the metal and the subsequent polarization of the ligand involves electron depopulation of the N–H bond, which culminates in a shift to lower energy [55]. At lower frequency, the complexes also exhibited a band near 470 cm^{-1} which is attributed to the *v*(Cu–N) vibration mode [56].

3.3. X-ray structure

X-ray single crystal diffraction analysis reveals that **1** crystallizes in the monoclinic space group $P2_1/c$. An ORTEP view of the compound is shown in figure 1 together with the numbering scheme. Selected bond lengths and angles are given in table 2.

The asymmetric unit of the complex is made up of a [LCu(μ-Cl)Cl]$_2$ dimeric unit with a lattice DMF. In the complex, *N*-(pyridin-2-ylmethyl)cyclohexanamine (L) is a neutral bidentate ligand which coordinates to copper(II) through its amine and pyridyl nitrogens. In addition, a terminal and a bridging

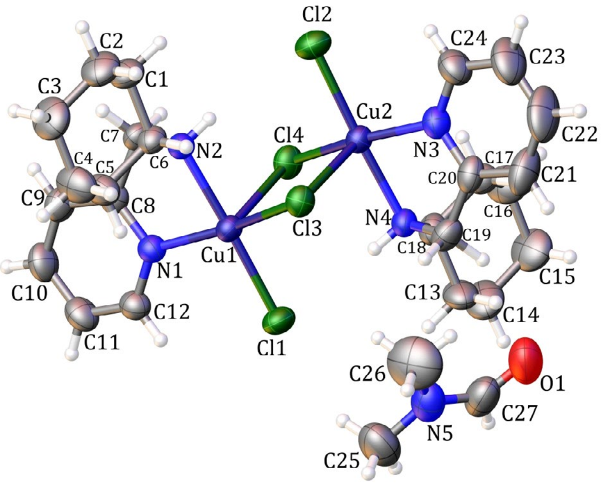

Figure 1. ORTEP view of [LCu(μ-Cl)Cl]$_2$ DMF (**1**). Thermal ellipsoids are drawn at the 50% probability level.

Table 2. Selected bond lengths (Å) and angles (°) for **1**.

Cu(1)–N(1)	2.009(2)	Cu(1)–N(2)	2.0471(18)
Cu(1)–Cl(1)	2.2536(8)	Cu(1)–Cl(3)	2.2905(7)
Cu(2)–N(3)	2.012(2)	Cu(2)–N(4)	2.0416(18)
Cu(2)–Cl(2)	2.2682(8)	Cu(2)–Cl(4)	2.2860(8)
Cu(2)–Cl(3)	2.7413(8)	Cu(1)–Cl(4)	2.8048(8)
Cu(1)–Cu(1)	3.3625(9)	Cl(3)–Cl(4)	3.8132(10)
Bond angles (°)			
N(1)–Cu(1)–N(2)	82.34(8)	N(1)–Cu(1)–Cl(1)	95.42(6)
N(1)–Cu(1)–Cl(4)	93.91(6)	N(1)–Cu(1)–Cl(3)	166.41(5)
N(2)–Cu(1)–Cl(4)	85.09(6)	N(2)–Cu(1)–Cl(1)	177.75(5)
N(2)–Cu(1)–Cl(3)	89.69(6)	Cl(1)–Cu(1)–Cl(3)	92.47(3)
Cl(1)–Cu(1)–Cl(4)	95.30(6)	Cl(3)–Cu(1)–Cl(4)	96.37(5)
N(3)–Cu(2)–N(4)	82.34(8)	N(3)–Cu(2)–Cl(2)	94.96(6)
N(3)–Cu(2)–Cl(4)	166.57(6)	N(3)–Cu(2)–Cl(3)	92.15(6)
N(4)–Cu(2)–Cl(4)	89.91(6)	N(4)–Cu(2)–Cl(3)	92.15(6)
N(3)–Cu(2)–Cl(2)	94.96(6)	Cl(2)–Cu(2)–Cl(3)	94.69(3)
Cl(2)–Cu(2)–Cl(4)	92.64(3)	Cl(3)–Cu(2)–Cl(4)	85.97(7)
Cu(1)–Cl(3)–Cu(2)	83.35(3)	Cu(1)–Cl(4)–Cu(2)	81.98(3)
Torsion angles (°)			
N(1)–C(8)–C(7)–N(2)	−24.4(3)	N(3)–C(20)–C(19)–N(4)	20.3(3)

chloride coordinate to copper(II). The complex consists of double chloride-bridged dimers, in which the bridging Cu_2Cl_2 unit is strictly planar due to the presence of the crystallographic inversion center in the middle of the dimer. The copper(II) is five-coordinate, being bonded to the bidentate ligand, and two bridging and one terminal chlorides. The bridging is unsymmetrical in nature with different Cu–Cl bond distances [Cu(1)–Cl(3) 2.2905(7) Å, Cu(1)–Cl(4) 2.8048(8) Å; Cu(2)–Cl(3) 2.7413(8) Å and Cu(2)–Cl(4) 2.2860(8) Å, table 2]. The fifth coordination site around each copper(II) is occupied by a terminal Cl(1) and Cl(2) ion with Cu(1)–Cl(1) and Cu(2)–Cl(2) distances of 2.2536(8) and 2.2682(8) Å, respectively. According to Addison *et al.* [57], the distortion of the square pyramidal geometry towards trigonal bipyramidal can be described by the geometrical parameter $\tau = |\beta - \alpha|/60$, where β and α are the bond angles involving the *trans* donors in the basal plane. The τ values for the coordination around the copper ions are 0.189 for Cu(1) Å and 0.178 for Cu(2) Å, confirming their distorted square pyramidal geometry. The bridging chlorides are in apical positions in each unit. The basal atoms are nearly coplanar; the deviations from the least squares plane through the CuN_2O_2 atoms are N(1) −0.106, N(2) 0.109, Cl(1) 0.086, Cl(3) −0.089, Cu(1) 0.107 Å and N(3) −0.103, N(4) 0.106, Cl(2) 0.083, Cl(4) −0.085, Cu(2) 0.110 Å. The two planes are almost parallel with an angle of 178.29°. The mean Cu–N(amine) distance of 2.03 Å and the bite angles N(1)–Cu(1)–N(2) and N(3)–Cu(2)–N(4) of 82.34(8)° are smaller than 90°, due to the strain caused by the three-bond ligand bite and are close to the corresponding average values of the copper(II) complexes with ethylenediamine [7]. The cyclohexyl groups are directed away from the $N_2CuCl_2CuN_2$ plane and to opposite sides of the terminal chlorides to minimize the steric hindrance around copper(II). Both five-membered chelate rings in the complex are puckered so that the torsion angles of N(1)–C(8)–C(7)–N(2) and N(3)–C(20)–C(19)–N(4) are 24.34(10)° and 20.35(10)°, respectively. Several dinuclear $[N_2Cu(\mu\text{-}Cl)]_2$ complexes are known in which two chloride ions are doubly bridging between the copper ions. Many of these compounds also have a distorted square pyramidal geometry about the copper ions, in which the apical position of one copper is occupied by chloride, which is equatorial to the other copper [29, 30, 37]. The reported Cu–N distances vary from 1.98 to 2.12 Å, the in-plane Cu–Cl distances differ from 2.19 to 2.31 Å, the axial Cu–Cl distances vary from 2.63 to 2.95 Å and the Cu···Cu distances differ from 3.42 to 3.74 Å. The Cu···Cu distance in **1** is 3.463(10) Å which lies between these values, but the Cu–Cl–Cu angles (81.98(3)° and 85.97(7)°) in $[LCu(\mu\text{-}Cl)Cl]_2$ are rather small compared with the Cu–Cl–Cu angles in the related compounds, which vary from 87.3° to 94.88°.

The geometry of the complex consists of two square pyramids sharing one base-to-apex edge (SP-I in scheme 3) [42]. Similar dinuclear copper(II) complexes having a $Cu(\mu\text{-}Cl)_2Cu$ core with square

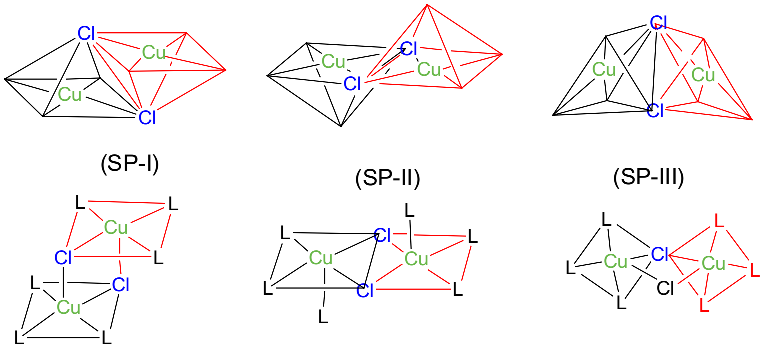

Scheme 3. Different conformations of dichloride-bridged, square-pyramidal dinuclear copper(II) complexes.

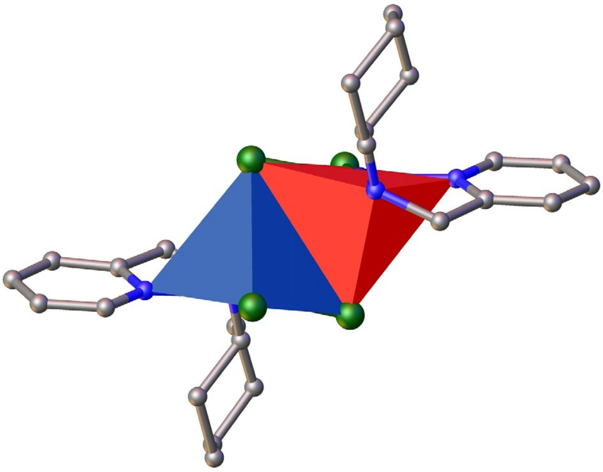

Figure 2. Arrangement of the two square pyramids of the two copper(II) centers showing the SP-I configuration in **1**.

pyramidal copper(II) centers and with nearly parallel basal planes are reported [13–17, 29–37, 39, 40, 58]. The cyclohexyl moieties are in chair conformations.

The crystal packing (figure 2) of the dimeric $[Cu(L)Cl]_2$ complex shows that the structure is stabilized by an intermolecular hydrogen bonding through DMF molecules in the lattice between the two dimeric $[LCu(\mu\text{-}Cl)Cl]_2$ complexes.

3.4. Electronic spectra

The visible electronic absorption spectra for **1** and **2** in dichloromethane solution show maxima at 672 and 686 nm, respectively, that are in agreement with those of five-coordinate copper(II) complexes with analogous geometries. Compound **2** shows a higher λ_{max} than **1**, signifying more distortion toward a trigonal bipyramid [59]. This spectral feature is characteristic of five-coordinate copper(II) complexes with distorted square pyramidal geometry that normally display a band in the 550–660 nm range (d_{xz}, $d_{yz} \rightarrow d_{x^2-y^2}$) [60, 61]. Moreover, **2** shows one strong ligand-to-metal charge transfer (LMCT) band at 475 nm [62]. The electronic spectra of both complexes show typical absorptions at 200–300 nm allocated to ligand $\pi \rightarrow \pi^*$ transitions.

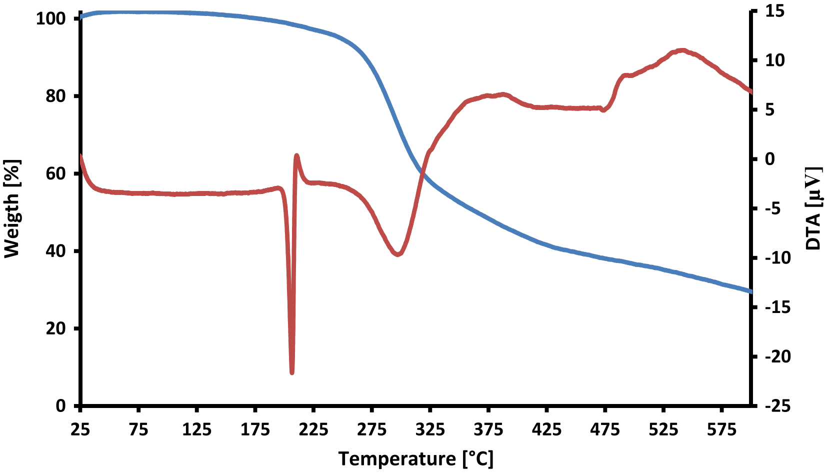

Figure 3. TGA and DTA curves for **1**.

3.5. Thermal analysis

Thermal stability and thermal behavior of the complexes were investigated by thermogravimetric analysis (TGA-DTA) in aerated atmosphere from 25 to 600 °C at a heating rate of 10 °C min^{-1}. Correlations between decomposition steps of the complexes with the corresponding weight losses are almost the same for **1** and **2**. The DTA curve of **1** (figure 3) indicates an endothermic process without any weight loss from 180 to 210 °C due to breakage of weak Cu–Cl in $[LCu(\mu\text{-}Cl)Cl]_2$ and formation of $2[LCuCl_2]$. The next endothermic process occurs at 230–470 °C associated with fragmentation and thermal degradation of the organic moiety and formation of $CuCl_2$ with mass loss of 38% (Calcd 38.6%).

3.6. Thermochromism

The compounds show irreversible thermochromism in the solid state which is reversible in solution. The original blue-green color of **1** turns to dark green upon heating to 130 °C in the solid state. The visible spectrum of **1** was studied over the temperature range of 25–170 °C in DMSO (figure 4). The complex

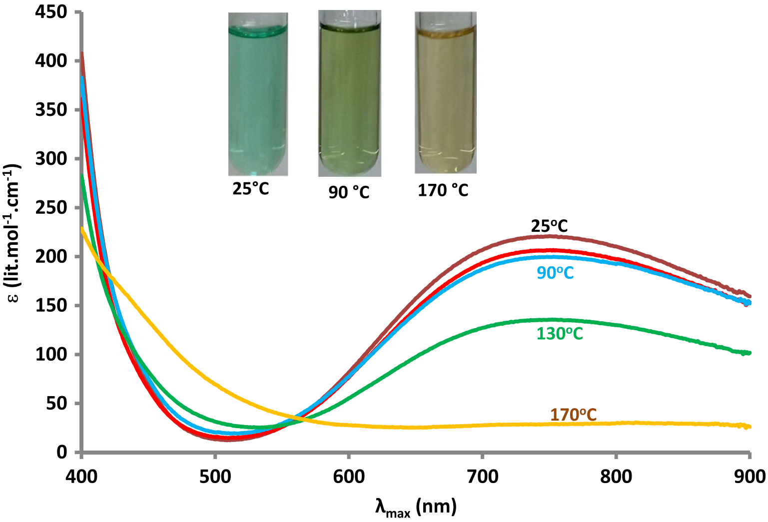

Figure 4. Temperature dependence of the visible absorbance of a DMSO solution of **1**.

demonstrates reversible thermochromism so that the original green color of the solution gradually turns to yellow-green up to 90 °C and to brown by increasing the temperature to 170 °C. The color change was attributed to the substitution of DMSO molecules with the coordinated diamine and chloride ligands. The observed brown color is due to the presence of free diamine ligand and $[Cu(dmso)_n]Cl_2$. This was confirmed by the comparison of the visible spectrum of the diamine ligand that was added to a heated solution of $CuCl_2$ in DMSO. This phenomenon is a reversible process so that after cooling the solution to room temperature the free diamine ligand and chloride ions that exist in the solution re-coordinate to the copper ions with reappearance of the original blue-green color. The reverse process is slower than the forward reaction and takes almost a day for full development of the original color due to tight bond formation between DMSO and Cu(II) and presence of a significant amount of solvent molecules around the copper centers. The same phenomenon was also observed in DMF solution. The reversible thermochromism was observed in **2** in the solvents DMSO and DMF with the same color change. However, in this case the reverse reaction takes only a few hours for the original color to reappear.

3.7. Solvatochromism

The complexes are soluble in a wide range of organic solvents and solvatochromic. The visible spectral variations of the complexes in various solvents are demonstrated in figure 5. The location of the absorption maxima of the complexes accompanied by their molar absorptivity values are compiled in table 3. The structures of the complexes are susceptible to changes in different solvents due to breaking of the weak Cu–Cl bond. In low polarity solvents, the dimeric structure of the compounds could dissociate into two mononuclear neutral complexes along with coordination of the solvent molecules to the vacant sites of the copper center (Route 1 in scheme 4), although, the solvation of the dimeric complexes cannot be ruled out. However, in solvents with medium polarity such as NB, MeOH, DMF, DMSO, and EtOH, not only do the dimeric complexes dissociate into two mononuclear complexes but also the weakly coordinated halide anion in the axial coordination site is displaced by solvent molecule due to Jahn-Teller effect of copper(II) ion with d^9 configuration (Route 2 in scheme 3). In aqueous solution, all coordinated halide ions are dissociated and replaced by water molecules (Route 3 in scheme 3). Therefore, both complexes demonstrated identical spectra in aqueous solution as shown in figure S2 in the Supplementary Material. The proposed mechanism is confirmed by changes in molar conductance values of the compounds in different solvents as shown in table 4. As a result, the color variations might be attributed to structural change followed by solvation of the resulting mononuclear complexes.

Table 3. The electronic absorption maxima of **1** and **2** in different solvents.

	Compound **1**		Compound **2**	
Solvent	λ_{max} (nm)	ε^a	λ_{max} (nm)	ε^a
1,2-DCE	672	445	686	490
DCM	712	164	728	472
NM	710	209	690	286
NB	719	283	693	392
AN	726	316	702	330
PN	693	335	717	458
Ac	670	370	665	680
H_2O	672	120	695	130
THF	752	294	747	277
EtOH	730	285	736	295
MeOH	725	219	731	311
DMF	788	253	779	295
DMSO	742	203	754	372
Py	776	384	871	479
HMPA	758	214	774	402

[a] ε (L cm^{-1} mol^{-1}).

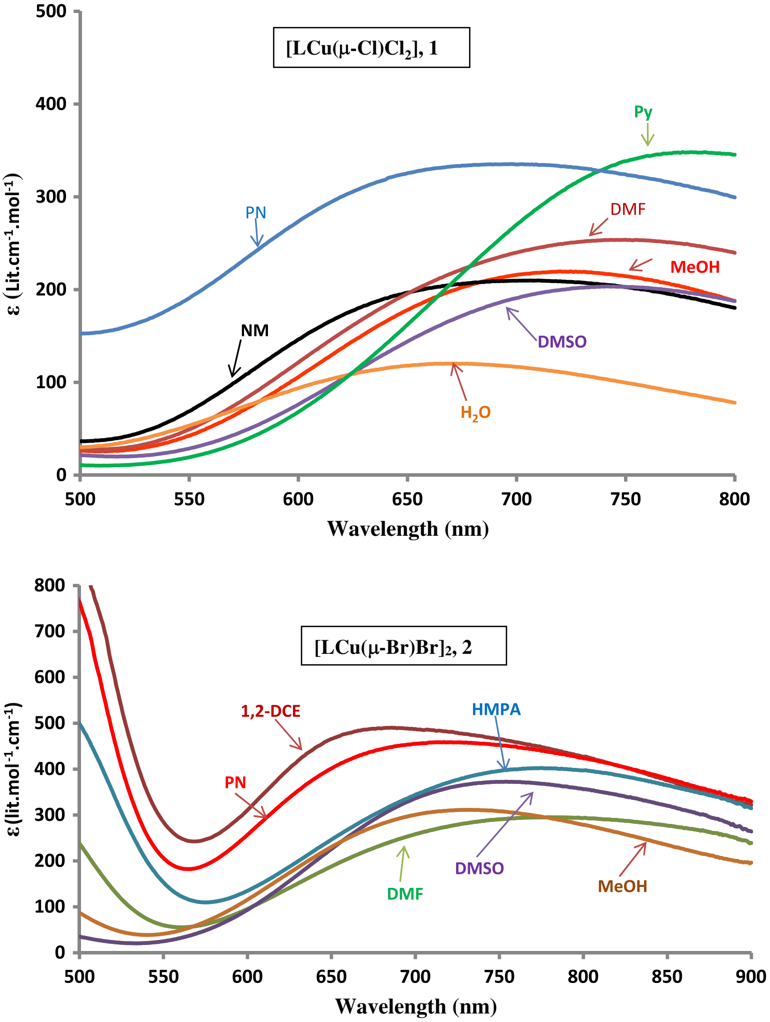

Figure 5. Absorption spectra of **1** and **2** in selected solvents. Absorption spectra in other solvents are omitted for clarity.

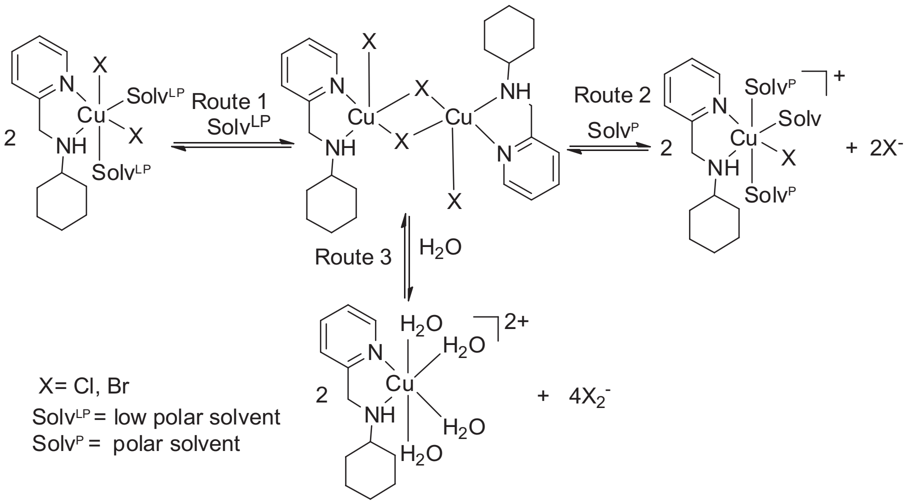

Scheme 4. Structural change of the complexes caused by solvents with different polarities.

Table 4. Molar conductivity data (Λ_m) of **1** and **2** (Ω^{-1} cm^2 mol^{-1}) at 25 °C in different solvents.

Complexes	NM	NB	AC	ACN	ETOH	MeOH	DMF	H_2O
Complex **1**	6	5	168	230	69	184	171	420
Complex **2**	8	11	182	244	71	214	153	428
1 : 1 electrolytes	75–95	20–30	100–140	120–160	35–45	80–115	65–90	118–131
1 : 2 electrolytes	150–180	50–60	160–200	220–300	70–90	160–220	130–170	235–273
1 : 3 electrolytes	220–260	70–80	–[a]	340–420	–[a]	–[a]	200–240	408–435

[a] The standard value is not reported.

3.8. Halochromism

In aqueous solution, the structure of the original dinuclear complexes collapses into two mononuclear complexes followed by hydration of the coordinated halide ions as shown in scheme 5. This structural change is accompanied with the change in the color of the complex from bluish green to blue in **1** and dark green to blue in **2**. This hydration causes an increase in the conductivity of the solution up to a 2 : 1 electrolyte. This phenomenon occurs in both complexes as evidenced by their identical electronic spectra in aqueous solution. The electronic absorption spectra of the complexes in aqueous solution are sensitive to pH, so that the original green color of the aqueous solution turns to blue upon addition of a base (NaOH, 0.1 M). This occurrence is totally reversible. To explore the color changes, the visible spectra of the complexes were studied from pH 5.7 (original pH) to 11. These results are shown in figure 6. There is an isosbestic point at 656 nm, which is visible in different pH scales. As the pH of the solution increased with addition of the base (NaOH, 0.1 M), the absorption bands shifted to lower wavelength due to deprotonation of the coordinated water molecules followed by deprotonation of amine group as shown in scheme 5. Spectrophotometric titration of the complex with NaOH showed release of six protons around pH 11 based on original $[LCu(\mu\text{-}X)X]_2$ complexes (figure 6). Interestingly, when the pH of the solution was decreased to 2.0 by addition of perchloric acid (0.1 M) the original blue color of the solution faded. The color lightening was accompanied by a red shift and decrease in intensity of the d–d band. The original blue color of the copper(II) complexes redeveloped upon increasing the pH of the solution to around 5 with addition of base.

Spectrophotometric titration of the original $[LCu(\mu\text{-}X)X]_2$ complexes with perchloric acid at λ_{max} = 706 nm (figure 7) demonstrated that the color lightening happened with consumption of four equivalents of proton. It is possibly because of protonation of the amine and pyridyl groups and formation of protonated ligand and formation of a fully hydrated copper(II) complex. In a complementary experiment, an aqueous solution of copper(II) perchlorate was acidified and the ligand L was then added

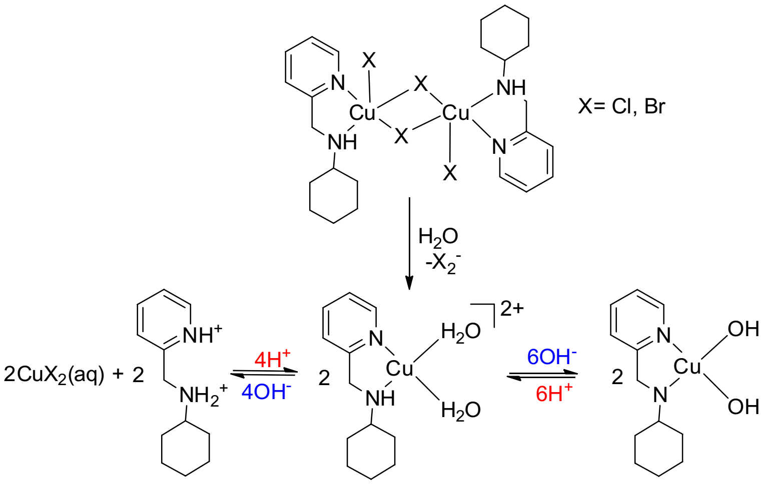

Scheme 5. Interconversion of complexes triggered by acid and base (pH 3–11.0) in aqueous solution.

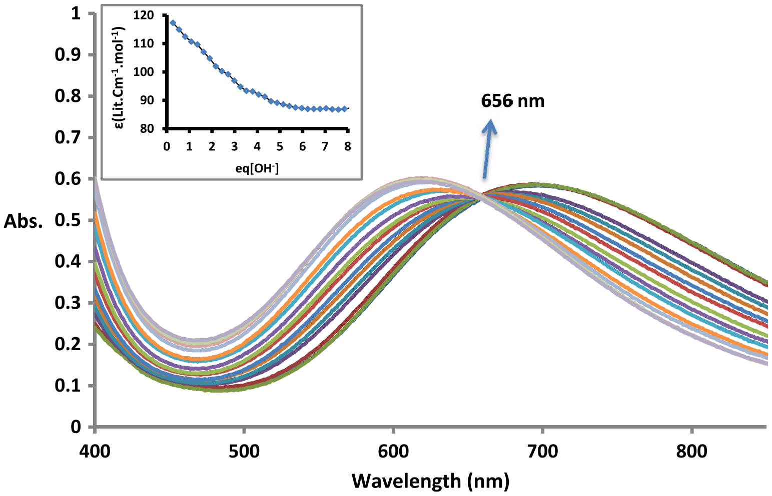

Figure 6. pH titration of $[LCu(\mu\text{-}Cl)Cl]_2$, **1**, and (4 mM in H_2O) with NaOH (0.10 M). The inset graph shows the decrease of 700 nm absorbance on titration of **1**, NaOH (0.10 M).

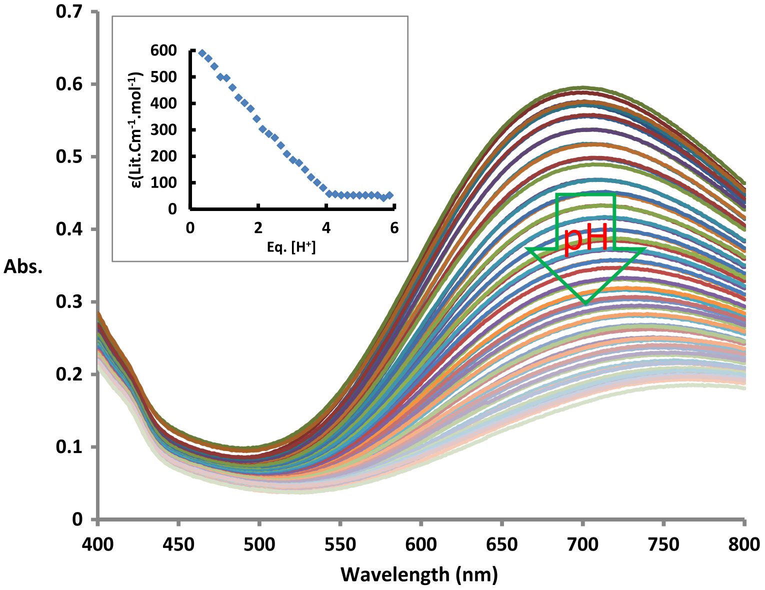

Figure 7. The pH-dependent visible spectrum of **1** in aqueous solution at 25 °C. The inset graph shows the decrease of 706 nm absorbance on titration of **1** (4 mM in H_2O) with $HClO_4$.

to the resultant solution. The blue color of the solution abruptly decolorized and the same spectrum as acidified $[LCu(\mu\text{-}X)X]_2$ was generated.

4. Conclusion

Dinuclear dichloro- and dibromo-bridged Cu(II) complexes with an N_2 chelating ligand were synthesized and characterized. The structure around copper(II) with N_2Cl_3 cores is distorted square pyramidal. The weakly coordinated halide ions can be replaced by donor solvents. The complexes are halochromic with reversible color change over the pH range 1.0–11.0, so that they can act as pH-induced off–on–off absorption switches through protonation and deprotonation of the coordinated ligand in aqueous solution. The compounds also demonstrate reversible thermochromism with distinct color changes from 25 to 170 °C in DMSO and DMF. The mechanism for this reversible color change is likely from removal and addition of the coordinated halides by solvent molecules. The complexes are soluble in a large number of organic solvents and solvatochromic. Their solvatochromism behaviors are due to structural change followed by solvation of the complexes. This work will be of value in terms of complexes which find their application as potential candidates for sensor materials and molecular switches.

Supplementary material

CCDC 1417858 contains the supplementary crystallographic data for this article. These data can be obtained free of charge via www.ccdc.cam.ac.uk/conts/retrieving.html or from the Cambridge Crystallographic Data Center, 12 Union Road, Cambridge CB2 1EZ, UK; Fax: (+44) 1223 336033; or E-mail: deposit@ccdc.cam.ac.uk. Supporting Information.

Disclosure statement

No potential conflict of interest was reported by the authors.

Funding

This work was supported by the University of Mazandaran of the Islamic Republic of Iran.

References

[1] Y. Fukuda. *Inorganic Chromotropism*, Springer, Berlin (2007).

[2] W. Linert, Y. Fukuda, A. Camard. *Coord. Chem. Rev.*, **218**, 113 (2001).

[3] P. Bamfield. *Chromic Phenomena: Technological Applications of Color Chemistry*, Springer Verlag, Berlin (2002), p. 8.

[4] M.S. Kryatova, O.V. Makhlynets, A.Y. Nazarenko, E.V. Rybak-Akimova. *Inorg. Chim. Acta*, **387**, 74 (2012).

[5] I. Lumb, M.S. Hundal, M. Corbella, V. Gómez, G. Hundal. *Eur. J. Inorg. Chem.*, 4799 (2013).

[6] H. Golchoubian, G. Moayyedi, N. Reisi. *Spectrochim. Acta, Part A*, **138**, 913 (2015).

[7] H. Golchoubian, M. Tarahomi, E. Rezaee, G. Bruno. *Polyhedron*, **85**, 635 (2015).

[8] H. Golchoubian, A. Heidarain, E. Rezaee, F. Nicolò. *Dyes Pigm.*, **104**, 175 (2014).

[9] J. Piromchom, N. Wannarit, J. Boonmak, C. Pakawatchai, S. Youngme. *Inorg. Chem. Commun.*, **40**, 59 (2014).

[10] A.A. Abou-Hussen, W. Linert. *Synth. React. Inorg. Met.-Org. Chem.*, **39**, 570 (2009).

[11] N. Baho, D. Zargarian. *Inorg. Chem.*, **46**, 7621 (2007).

[12] D. Venegas-Yazigi, D. Aravena, E. Spodine, E. Ruiz, S. Alvarez. *Coord. Chem. Rev.*, **254**, 2086 (2010).

[13] S. Choubey, S. Roy, S. Chattopadhayay, K. Bhar, J. Ribas, M. Monfort, B.K. Ghosh. *Polyhedron*, **89**, 39 (2015).

[14] S. Thakurta, P. Roy, G. Rosair, C.J. Gómez-García, E. Garribba, S. Mitra. *Polyhedron*, **28**, 695 (2009).

[15] K. Skorda, T.C. Stamatatos, A.P. Vafiadis, A.T. Lithoxoidou, A. Terzis, S.P. Perlepes, J. Mrozinski, C.P. Raptopoulou, J.C. Plakatouras, E.G. Bakalbassis. *Inorg. Chim. Acta*, **358**, 565 (2005).

[16] T. Rojo, M.I. Arriortua, J. Ruiz, J. Darriet, G. Villeneuve, D. Beltran-Porter. *J. Chem. Soc., Dalton Trans.*, 285 (1987).

[17] I. Banerjee, P.N. Samanta, K.K. Das, R. Ababei, M. Kalisz, A. Girard, C. Mathoniere, E.D. Estes, W.E. Estes, W.E. Hatfield, D.J. Hodgson. *Inorg. Chem.*, **14**, 106 (1975).

[18] J. Xiang, Q. Li, P. Mei. *Acta Crystallogr., Sect. E*, **62**, m2348 (2006).

[19] S. Zhang, W. Chen, B. Hu, Y. Chen, L. Zheng, Y. Li, W. Li. *J. Coord. Chem.*, **65**, 4147 (2012).

[20] S.-S. Qian, Y. Lu, Z.-L. You, H.-L. Zhu. *Synth. React. Inorg. Met. Org. Nano-Met. Chem.*, **43**, 107 (2013).

[21] R. Kapoor, A. Kataria, P. Venugopalan, P. Kapoor, M. Corbella, M. Rodríguez, I. Romero, A. Llobet. *Inorg. Chem.*, **43**, 6699 (2004).

[22] Y.-M. Lee, H.-W. Lee, Y.-I. Kim. *Polyhedron*, **24**, 377 (2005).

[23] M. Rodríguez, A. Llobet, M. Corbella, A.E. Martell. *Inorg. Chem.*, **38**, 2328 (1999).

[24] A. Colombo, L. Menabue, A. Motori, G.C. Pellacani, W. Porzio, F. Sandrolini, R.D. Willett. *Inorg. Chem.*, **24**, 2900 (1985).

[25] S.G.N. Roundhill, D.M. Roundhill, D.R. Bloomquist, C. Landee, R.D. Willett, D.M. Dooley, H.B. Gray. *Inorg. Chem.*, **18**, 831 (1979).

[26] B. Scott, U. Geiser, R.D. Willett, B. Patyal, C.P. Landee, R.E. Greeney, T. Manfredini, G.C. Pellacani, A.B. Bonamartini Corradi, L.P. Battaglia. *Inorg. Chem.*, **27**, 2454 (1988).

[27] P. Kapoor, A.P.S. Pannu, M. Sharma, M.S. Hundal, R. Kapoor, M. Corbella, N. Aliaga-Alcalde. *J. Mol. Struct.*, **981**, 40 (2010).

[28] I. Lumb, M.S. Hundal, M. Corbella, V. Gomez, G. Hundal. *Eur. J. Inorg. Chem.*, 4799 (2013).
[29] D.W. Phelps, W.H. Goodman, D.J. Hodgson. *Inorg. Chem.*, **15**, 2266 (1976).
[30] D.D. Swank, G.F. Needham, R.D. Willett. *Inorg. Chem.*, **18**, 761 (1979).
[31] M. Nethaji, R. Clerac, M. Ali. *Dalton Trans.*, **42**, 1879 (2013).
[32] S.J. Brown, X. Tao, T.A. Wark, D.W. Stephan, P.K. Mascharak. *Inorg. Chem.*, **27**, 1581 (1988).
[33] F. Tuna, L. Patron, Y. Journaux, M. Andruh, W. Plass, J.C. Trombe. *J. Chem. Soc., Dalton Trans.*, 539 (1999).
[34] X.H. Bu, M. Du, Z.L. Shang, L. Zhang, Q.H. Zhao, R.H. Zhang, M. Shionoya. *Eur. J. Inorg. Chem.*, 1551 (2001).
[35] X.H. Bu, M. Du, L. Zhang, Z.L. Shang, R.H. Zhang, M. Shionoya. *J. Chem. Soc., Dalton Trans.*, 729 (2001).
[36] M. Du, Y.M. Guo, X.H. Bu, J. Ribas, M. Monfort. *New J. Chem.*, **26**, 645 (2002).
[37] A.M. Schuitema, A.F. Stassen, W.L. Driessen. *Inorg. Chim. Acta*, **337**, 48 (2002).
[38] A. Bernalte-García, A.M. Lozano-Vila, F. Luna-Giles, R. Pedrero-Marín. *Polyhedron*, **25**, 1399 (2006).
[39] H.W. Lee, N. Sengottuvelan, H.-J. Seo, J.S. Choi, S.K. Kang, Y.-I. Kim. *Bull. Korean Chem. Soc.*, **29**, 1711 (2008).
[40] F. Yraola, F. Albericio, M. Corbella, M. Royo. *Inorg. Chim. Acta*, **361**, 2455 (2008).
[41] A. Višnjevac, L. Tušek-Bozic, M. Majeric-Elenkov, V. Šunjic, B. Kojic-Prodic. *Eur. J. Inorg. Chem.*, 2647 (2001).
[42] E. Gungor, H. Kara. *Inorg. Chim. Acta*, **384**, 137 (2012).
[43] H. Grove, J. Sletten, M. Julve, F. Lloret. *J. Chem. Soc., Dalton Trans.*, 1029 (2001).
[44] J.A. Carrabine, M. Sundaralingam. *J. Am. Chem. Soc.*, **92**, 369 (1970).
[45] R.F. Drake, V.H. Crawford, N.W. Laney, W.E. Hatfield. *Inorg. Chem.*, **13**, 1246 (1974).
[46] D.J. Hodgson, E. Pedersen. *Acta Chem. Scand., Ser. A*, **36a**, 281 (1982).
[47] W.E. Marsh, K.C. Patel, W.E. Hatfield, D.J. Hodgson. *Inorg. Chem.*, **22**, 511 (1983).
[48] A. Nielsen, S. Veltzé, A.D. Bond, C.J. McKenzie. *Polyhedron*, **26**, 1649 (2007).
[49] G.A. van Albada, O. Roubeau, P. Gamez, H. Kooijman, A.L. Spek. *Inorg. Chim. Acta*, **357**, 4522 (2004).
[50] X-AREA. *Version 1.30, Program for the Acquisition and Analysis of Data*, Stoe & Cie GmbH, Darmstadt, Germany (2005).
[51] X-SHAPE. *Version 2.05, Program for Crystal Optimization for Numerical Absorption Correction*, Stoe & Cie GmbH, Darmstadt, Germany (2004).
[52] X-RED. *Version 1.28b, Program for Data Reduction and Absorption Correction*, Stoe & Cie GmbH, Darmstadt, Germany (2005).
[53] M.C. Burla, R. Caliandro, M. Camalli, B. Carrozzini, G.L. Cascarano, L. De Caro, C. Giacovazzo, G. Polidori, R. Spagna. *J. Appl. Crystallogr.*, **38**, 381 (2005).
[54] G.M. Sheldrick. *Acta Cryst.*, **64**, 112 (2008).
[55] C. Tsiamis, M. Themeli. *Inorg. Chim. Acta*, **206**, 105 (1993).
[56] N. Raman, S. Esthar, C. Thangaraja. *J. Chem. Sci.*, **116**, 209 (2004).
[57] A.W. Addison, T.N. Rao, J. Reedijk, J. van Rijn, G.C. Verschoor. *J. Chem. Soc., Dalton Trans.*, 1349 (1984).
[58] H. Liu, F. Gao, D. Niu. *Inorg. Chim. Acta*, **362**, 4179 (2009).
[59] S.J. Brudenell, L. Spiccia, E.R.T. Tiekink. *Inorg. Chem.*, **35**, 1974 (1996).
[60] G.A. McLachlan, G.D. Fallon, R.E. Martin, L. Spiccia. *Inorg. Chem.*, **34**, 254 (1995).
[61] M. Yonemura, K. Arimura, K. Inoue, N. Usuki, M. Ohba, H. Ōkawa. *Inorg. Chem.*, **41**, 582 (2002).
[62] T.M. Donlevy, L.R. Gahan, T.W. Hambley, G.R. Hanson, K.L. McMahon, R. Stranger. *Inorg. Chem.*, **33**, 5131 (1994).